Subsurface Flow Batteries: Concept, Benefits and Hurdles

D Waltham[1*], K B Holt[2], S Kuenzel[3], A Basu[1], N Lecoeur[1]

1. Department of Earth Sciences, Royal Holloway, Egham, Surrey TW20 0EX, UK

2. Department of Chemistry, University College London, London WC1H OAJ, UK

3. Department of Electrical Engineering, Royal Holloway, Egham, Surrey TW20 0EX, UK

Email: D.Waltham@rhul.ac.uk

Abstract: Storage of flow-battery electrolytes in aquifers is a novel concept for storing electrical energy in the subsurface. Flow-batteries operate by electrochemical transformations of electrolytes, rather than of electrodes, and their energy capacity can therefore be increased indefinitely by using larger electrolyte tanks. Saline aquifers may be the cheapest way to provide large-scale storage for this purpose. Storage would be within high-porosity, high-permeability reservoirs sealed by impermeable layers but—in contrast to hydrocarbon, H_2 or CO_2 storage—electrolytes would be trapped in lows (rather than highs) of such formations as a consequence of their high density compared to natural brines.

We investigate a range of electrochemical, geochemical, microbiological and engineering hurdles which must be overcome if subsurface flow-batteries are to become a practical technology. No insurmountable problems were found but further laboratory studies are needed. Our economic assessment suggests that subsurface flow batteries should be more cost effective than hydrogen-based power-to-gas approaches for discharge/charge timescales of around a day but that hydrogen will be cheaper for longer-term storage. Hence, meeting future energy-storage needs may involve a combination of both approaches.

A non-peer-reviewed preprint submitted to EarthArXiv. MS is in review for a Special Publication of the Geological Society of London.

Introduction

This paper considers a novel proposal for storage of electricity (specifically, storing electrochemically active fluids within subsurface, porous reservoirs). We begin by looking at why energy needs to be stored at all so that we can discuss where our proposal might find a niche in the spectrum of storage technologies.

The need for storage arises because electricity supply rarely matches demand. Demand fluctuates through the day, as consumer and industrial needs cycle up and down, and fluctuates over the seasons as the need for heating and cooling changes with the weather. Increasingly—as intermittent, renewable energy generates a growing fraction of total electricity—supply also fluctuates because the sun doesn't always shine and the wind doesn't always blow.

The supply/demand mismatch can occur on timescales from seconds to months and causes a range of different problems summarised in Table 1 (adapted from Schmidt et al, 2019). The table consists of rows showing different benefits of storage and columns showing different methods of storage.

	Pumped Hydro	Compressed Air	Flywheel	Li-ion	Sodium-Sulphur	Lead Acid	Vanadium Flow	Hydrogen	Super capacitor
Frequency & voltage control			x	x	x	x	x	x	x
Load balancing	x	x	x	x	x	x	x	x	x
Peaker replacement	x	x		x	x	x	x	x	
Seasonal storage	x	x					x	x	
Congestion management	x	x		x	x	x	x	x	

Table 1. Reasons for balancing electricity supply/demand and technologies for achieving balance (adapted from Schmidt et al, 2019)

A review of energy storage methods can be found in IRENA (2017) and readers are directed there for further details but, in outline, the approaches tabulated in Table 1 are as follows:

i. In pumped hydroelectric storage (PHS) excess electricity is used to pump water from a low reservoir to a higher one. Then, when demand exceeds supply, the water is transferred back from the higher reservoir to the lower via a turbine.
ii. Compressed air energy storage (CAES) involves using excess energy to pressurise air which is then stored in tanks or in salt caverns. When additional supply is needed, the pressurised air is used to drive a turbine.
iii. Flywheels speed up when "charging" using a machine as motor to convert electrical energy to kinetic energy whilst they generate electric power by converting the stored kinetic energy when "discharging". They can respond to demand/supply mismatch within seconds but do not have large energy capacity.
iv. The next four columns in Table 1 refer to different kinds of electrochemical battery. Li-Ion batteries, for example, are familiar as the usual battery type used in portable electronic devices and in electric vehicles. The fourth battery type, vanadium flow batteries, will be discussed in greater detail below as flow batteries are the central topic of this paper.
v. Hydrogen storage is the topic of many papers in this special volume and is the approach with the greatest similarities in technology and application to our proposal of subsurface electrolyte storage. Hydrogen storage involves using excess electricity to produce hydrogen, by electrolysis, and then regenerating electricity when required by either burning the hydrogen in a turbine or by using a hydrogen fuel cell. The hydrogen can be stored in tanks or stored underground in salt caverns, depleted hydrocarbon fields or in aquifers.

vi. The final storage approach, supercapacitors, is the only one which involves storage of electricity as electricity (rather than converting it to gravitational, kinetic, pressure or chemical energy). A supercapacitor is simply a capacitor with very high energy capacity (NB ordinary capacitors, as found in electronic circuits, only store microjoules of energy). Like flywheels, supercapacitors respond very quickly but are unable to store the large amounts of energy required for longer timescale applications.

Turning now to the rows in table 1, the first four benefits are broadly given in order of increasing timescale. The timescale boundaries between these benefits are arbitrary and blurred but it is nevertheless useful to divide them up in this way. In turn, these benefits are:

i. Frequency and voltage instabilities occur almost instantly when supply does not match demand. Handling this issue does not require large energy capacity but it does require a rapid response within seconds.
ii. Load balancing refers to managing short term power mismatches on timescales of minutes. On these timescales it is not possible to simply turn on and off additional generation capacity (see peaker plants, below). Hence, approaches are required that respond and provide/consume electricity on time scales longer than those used for frequency stabilization but shorter than the time for peaker plant activation/deactivation.
iii. Peaker replacement refers to replacing "peaker plants" (currently usually medium sized gas-fired turbines) that provide (relatively expensive) supplies when demand is high (e.g. for a few hours in the evenings).
iv. Seasonal balancing is the issue of providing sufficient power to cope with higher demand on timescales of weeks or months (e.g. for heating during winter).
v. Congestion management refers to longer term (hours to days) control of the consequences of too much, rather than too little, energy supply. For example, on windy summer days there may be more renewable energy than the grid requires. At present this is often managed by closing down wind farms but this is not a good use of expensive infrastructure. Storage of the excess would be a better solution.

With this background it can be seen that some energy storage approaches (e.g. flywheels and supercapacitors) are more useful for rapid/low-capacity applications whilst others (e.g. CAES and PHS) are more useful for slow/high-capacity applications.

This paper's proposal, to store energy electrochemically in the subsurface, is likely to be similar to CAES, H_2 storage and PHS in terms of the speed with which it can be accessed. We'll also show, later, that it will be similar to PHS in terms of capacity. It is therefore useful to add a little more detail about the power and capacity of typical PHS storage as this is the approach that might be most directly replaced by electrolyte storage.

At present, most of the global electricity storage capacity is in the form of pumped hydroelectric storage. The largest existing PHS plant, in the UK, is the Dinorwig Power Station in north Wales with an energy storage capacity of 9.1 GWh at a maximum power of 1.7 GW (Scottish Renewables 2016). Hence, this system can store or release electricity, at maximum power, for 9.1/1.7=5.4 hours. The planned Coire-Glas PHS project in Scotland will have slightly lower power (1.5 GW) but a capacity of 30-40 GWh (ibid) thus giving a discharge/charge time, at maximum power, of 20-27 hours.

However, PHS systems are confined to mountainous geographical locations which are often remote from electricity generators and users. Furthermore, building the numbers of PHS systems that will be required, as the renewable energy share of generation increases, is simply not practical. For

example, the IEA (2009) projects that the need for additional electrical storage may be as high as 90GW in Western Europe alone by 2050, i.e. 60 storage facilities as large as Coire-Glas. It is unlikely that enough suitable sites can be found and additional ways of storing electrical energy on PHS-like timescales will be needed.

Subsurface hydrogen storage and/or compressed-air energy storage (CAES) may be good PHS replacements but this paper investigates, for the first time, whether subsurface flow batteries (SFBs) should also be considered.

Flow batteries differ from traditional batteries by using electrochemical transformations of (two separate) electrolytes rather than of electrodes (Park *et al.* 2016)(see later for more details). As a consequence, they can provide high energy-capacity at low cost if large, cheap electrolyte tanks are available. This paper considers whether porous-rock reservoirs are suitable storage locations (see Fig. 1). In this concept, electrolytes are pumped out at one end of their respective reservoirs, through the flow-battery and back into the opposite end of their reservoirs during charging. The flow direction is reversed during discharging. Hence, the volume of electrolyte in each reservoir is kept constant (ignoring small changes in volume associated with chemical and physical alterations of the electrolytes).

This concept of electrolyte storage in porous reservoirs is novel although energy companies are considering storage of electrolytes in salt caverns (EWE, 2017; RWE, 2020).

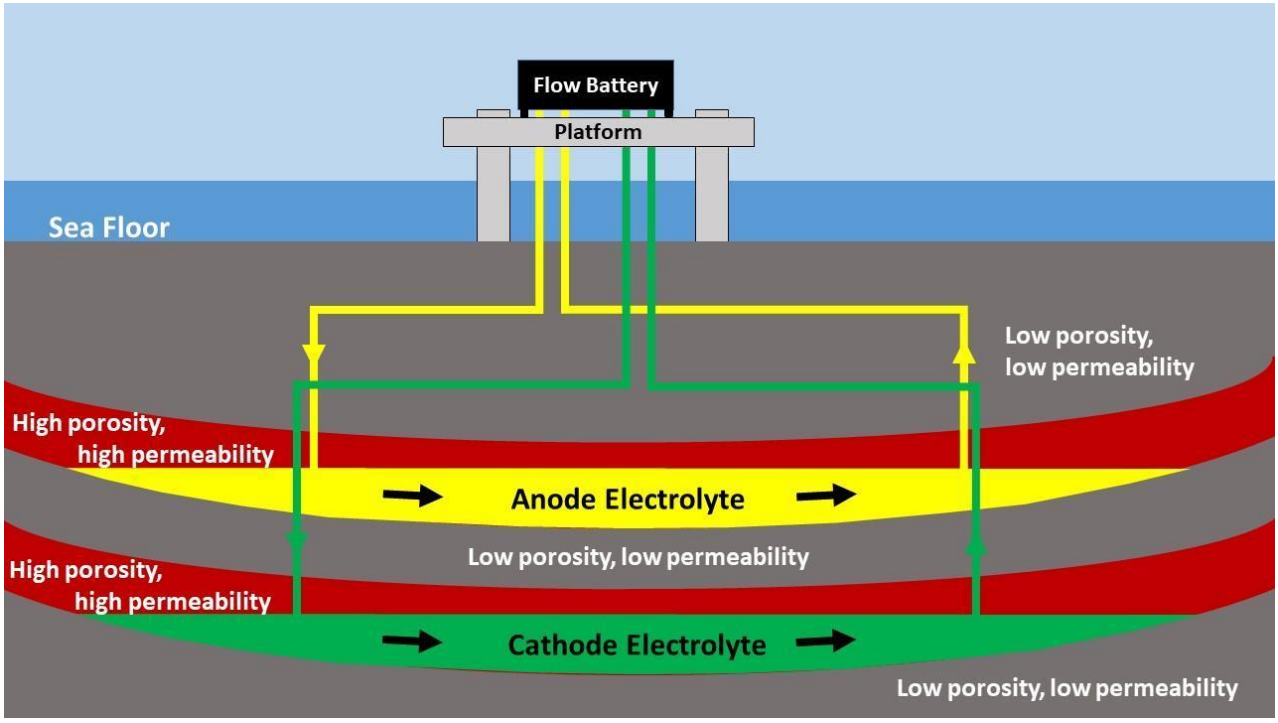

Figure 1. The subsurface flow-battery concept. Low-cost, high-capacity electrolyte storage is provided by porous reservoirs. Electrolyte density will be higher than that of natural brines and, hence, storage will be at the base of the reservoirs with an underlying “cap” rock.

The next section provides a brief introduction to flow batteries for the benefit of readers who may be unfamiliar with this technology. Then we look at the theoretical storage capacity and charge/discharge power that might be achieved by subsurface flow batteries. This is followed by a discussion of various electrochemical, geochemical, microbiological and engineering hurdles that must be overcome if SFBs are to become a practical technology. We finish with a look at costs

compared to other electrical storage technologies. Hence, this paper gives an initial assessment of whether SFBs could be technically, environmentally and economically viable.

Flow Batteries

Flow batteries were first developed by NASA in the 1970s but they are not yet sufficiently widespread that we can assume familiarity outside the field of electrochemistry. Hence, we include a brief summary here. For further information, readers are directed to our main source for this overview (Weber, 2011).

As stated above, the key characteristic of flow batteries is that the electrochemical transformations, that generate and store electricity, take place in liquid electrolytes whilst the electrodes remain unaltered. Conventional batteries are the exact opposite; they involve chemical transformations of electrodes mediated by a passive electrolyte.

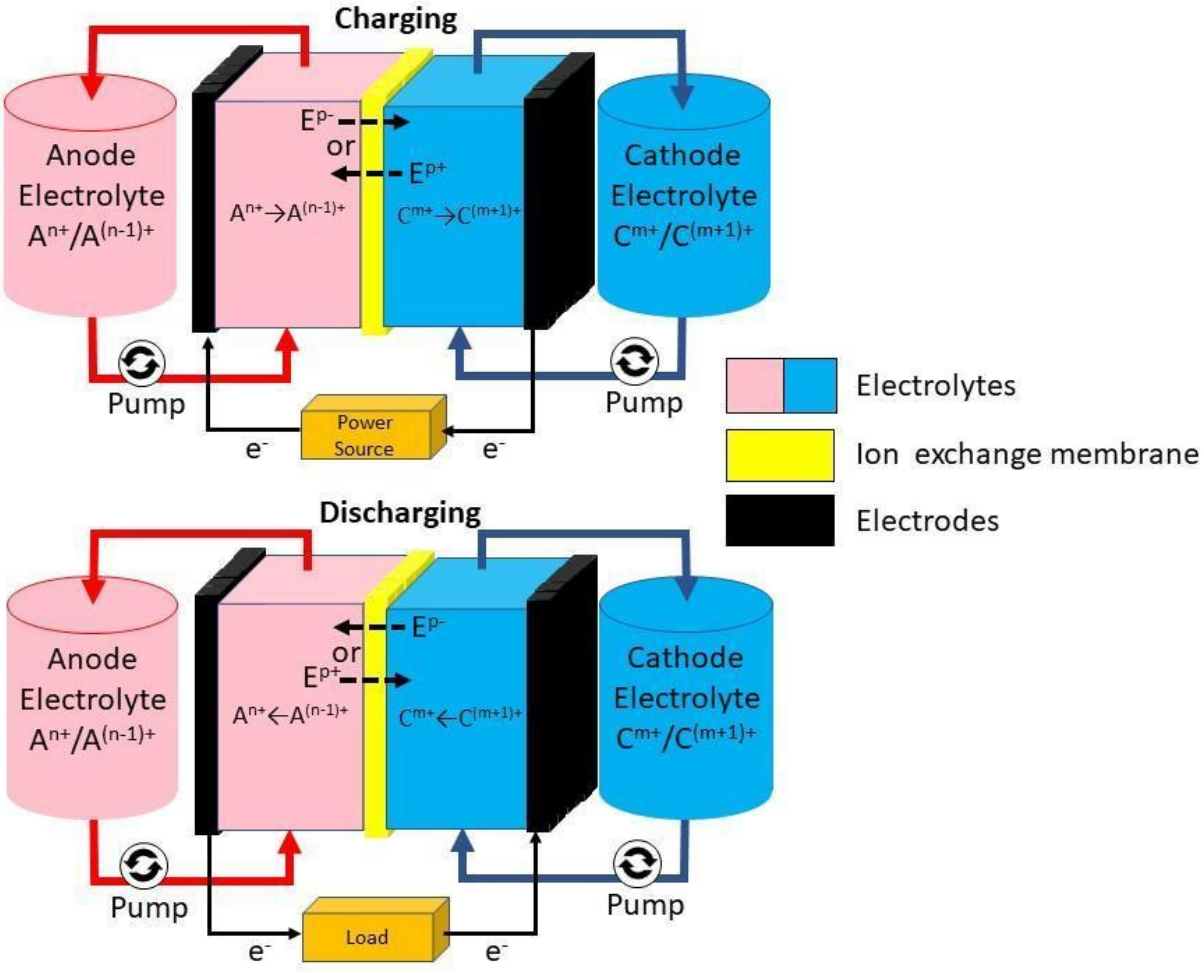

Figure 2. Operation and architecture of a generic flow battery. Upper diagram shows transformations and ion/electron flow during battery charging. Lower diagram shows these reversed during discharging. See text for further details.

Figure 2 illustrates the generic operation of a rechargeable flow battery. Unlike a conventional battery, there are two distinct electrolytes, i.e. an anode electrolyte initially containing A^{n+} cations and a cathode electrolyte initially consisting of C^{m+} cations (where A and C are chemical species and

m and n are small integers). The anode/cathode convention is potentially confusing in rechargeable batteries but, here, we use the convention that the cathode produces electrons during charging.

During charging, electron flow allows $A^{n+} \rightarrow A^{(n-1)+}$ (by addition of electrons) and $C^{m+} \rightarrow C^{(m+1)+}$ (by removal of electrons). Overall charge balance in the electrolytes is maintained by exchange of ions across a membrane. Exchange ions, E, can be negatively or positively charged and will flow from the anode to the cathode if negative, but from cathode to anode if positive. The transformations of A and C, and the flow of E across the membrane, are reversed if the battery is discharged rather than charged. Note that, except when fully charged or discharged, the anode and cathode electrolyte tanks contain a mixture of $A^{n+}/A^{(n-1)+}$ and $C^{m+}/C^{(m+1)+}$ respectively.

The architecture of the flow battery consists of a "stack" (i.e. the central cell containing the electrodes, membrane and reacting electrolytes) and external tanks containing the bulk of the electrolytes. This architecture leads to the key benefit of the flow-battery design; it separates power (rate of energy output or storage) from capacity (maximum amount of energy stored). Specifically, the power of the system is increased by having more stacks (or a bigger membrane/electrode area in the stack), whereas the capacity is increased by having larger external tanks.

The electrolytes must, of course, also contain cations (which may, or may not, be the same as the exchange ions that cross the membrane). The resulting electrolytes can also be water based or use a non-aqueous solvent. Hence—given the wide range of possible anions, cations, exchange ions and solvents—flow batteries can be constructed using a large number of different chemical systems. In this paper we concentrate upon the all-iron design of flow battery (Hruska and Savinell 1981).

The chemical reactions in the two halves of a discharging all-iron cell are

$$2FeCl_3 + 2e^- \rightarrow 2FeCl_2 + 2Cl^- \quad (1)$$

$$Fe + 2Cl^- \rightarrow FeCl_2 + 2e^- \quad (2)$$

The first reaction occurs within a mixed $FeCl_3/FeCl_2$ aqueous electrolyte whilst the second reaction involves dissolution of an iron-electrode into an $FeCl_2$ aqueous electrolyte. The chloride ions generated in reaction (1) diffuse across the ion exchange membrane to provide the chloride ions consumed in reaction (2).

"All-iron" refers to having iron compounds in both halves of the cell (i.e. A and C in Fig. 2 are both iron species). This reduces the amount, and impact, of diffusion across the membrane of iron ions. In general, it is not possible to restrict ion exchange only to the desired exchange ions but exchange of any other electrolyte ions is undesirable as it reduces the recovered energy and alters electrolyte compositions.

Hruska and Savinell (1981) give the voltage of the resulting cell as 1.21V and estimate the charge density of the electrolyte at 63.5 Ah/l. Hence, the theoretical energy density is 1.21 x 63.5 = 76.8 Wh/l (or, equivalently, $kWhm^{-3}$). This is probably close to the maximum upper limit since Hruska and Savinell (ibid) assumed a highly concentrated iron-chloride solution (500 g/l $FeCl_3$ ~ 6M). Note that this concentration is four orders of magnitude higher than the median iron concentration of 21 mg/L (range 0.1 - 985 mg/L, n = 100) reported in North Sea formation water (Warren et al., 1994). The energy density of the electrolytes is a key parameter since it will control the maximum amount of energy that can be stored in a reservoir of a given size and the maximum charge/discharge power for a given electrolyte pumping rate. We will put numbers on these quantities later in this paper.

An alternative all-iron design involves sulphate as the cation rather than chloride (Tucker et al, 2015; Yu et al 2021). This reduces problems with chlorides (principally highly corrosive electrolytes and problems with membrane longevity) but at the cost of lower-solubility and, hence lower concentration and energy density.

Note that, since the all-iron design involves dissolution and re-plating of an iron-electrode, it is a hybrid rather than pure flow battery. However, there are good reasons for choosing the all-iron configuration. Ferrous ions, sulphate ions and chloride ions are common constituents of subsurface brines (e.g. see Munz et al., 2010) and, hence, this particular flow battery chemistry is environmentally benign. Iron chlorides and sulphates are also low cost and widely available at industrial volumes. Iron chloride is particularly low cost as it is a by-product of the steel industry (Narayan et al, 2019).

Low cost and low environmental impact are our main reasons for focussing on the all-iron flow-battery in this preliminary assessment of SFBs. However most of our conclusions apply, or can be extended, to other flow battery designs. Common alternatives are an all-Vanadium design (the most technically developed flow battery at present but with expensive, toxic electrolytes), an iron-chromium design (which suffers from iron and chromium leakage across the membrane), a bromine-polysulphide design (which is prone to generating toxic HS and Br_2 gases), zinc-bromine (with similar issues due to HBr and Br_2) and a range of non-aqueous systems (which suffer from low electrolyte conductivity and high cost).

Theoretical Subsurface Flow Battery Performance

For illustrative convenience the two electrolytes in a subsurface flow battery are shown, in Fig. 1, as separated vertically. However, horizontal separation within multiple synclines of the same formation is also possible. The electrolytes will have high ion concentrations (compared to natural brines) in order to store significant energy and, hence, they will be relatively dense and sink to the base of the reservoir formation (as shown in Fig. 1). This leads to the first advantage of SFBs; electrolyte storage will be in synclinal structures sealed by underlying low-permeability formations. In contrast, CO_2 and H_2 subsurface storage are in anticlinal structures and so SFBs will not compete for the same storage locations. Furthermore, accidental leakage can be contained simply by shutting the pumping system down allowing dispersion of environmentally ubiquitous ions into the deeper subsurface.

However, SFBs are only useful if they can store/discharge electricity at high enough power. Furthermore, if they are to be used for longer-term storage, they must have a large energy-storage capacity. A combination of potential-flow theory and Darcy's law allows a first pass estimate of these quantities. This approach has been widely used to model subsurface flows for many decades (e.g. see King Hubbert, 1957).

Potential-flow theory assumes that slow, steady flows are irrotational and, hence, that velocity can be represented as the gradient of a potential field, i.e.

$$\mathbf{u} = \nabla \Phi \qquad (3)$$

where $\mathbf{u}$ is the flow velocity and Φ is potential. The simplified case of simultaneous injection and extraction of electrolyte using two perforated, vertical wells in a horizontal layer—of constant thickness, porosity and permeability—can then be modelled as a 2-dimensional potential flow, from a point source into a point sink, with a potential of

$$\Phi = (Q/4\pi) \ln[((x+a)^2 + y^2) / ((x-a)^2 + y^2)] \quad (4)$$

for a source at location x=-a, y=0 and a sink at location x=+a, y=0. Here, Q is the sink and source strength given by

$$Q = F/\varphi h \quad (5)$$

where F is the volume flux (m^3/s), φ is porosity and h is layer thickness. Note that this first attempt at quantification assumes there is no regional flow. Any strong regional flow would remove electrolyte from the storage location and should therefore be avoided.

An alternate formulation (Darcy-flow of a viscous fluid through a porous medium) gives a flow velocity of

$$\mathbf{u} = (-k/\mu\varphi)\nabla P. \quad (6)$$

Here, k is permeability, μ is viscosity and P is pressure. Comparison of eqns (3) and (6) then implies

$$P = (-\mu\varphi/k)\Phi + P_b \quad (7)$$

where P_b is a background pressure. Combining eqns (4), (5) and (7) gives the excess pressure field as

$$\Delta P = P - P_b = -(\mu F/4\pi kh) \ln[((x+a)^2 + y^2) / ((x-a)^2 + y^2)]. \quad (8)$$

The injection pressure is the excess pressure at the injection well radius, r_w, i.e. where

$$(x+a)^2 + y^2 = r_w^2. \quad (9)$$

Hence, the excess pressure around the injection well is

$$\Delta P = -(\mu F/4\pi kh) \ln[r_w^2/ (r_w^2 - 4ax)]. \quad (10)$$

But $r_w << a$ and $x \approx -a$. Hence,

$$\Delta P = (\mu F/4\pi kh) \ln[4a^2 / r_w^2]. \quad (11)$$

The key quantity in this expression is the volume-flux, F. This flux can be combined with the energy density, ρ_e, to give the device power. This energy density is defined, for electrochemical devices, as the maximum energy stored divided by the volume of the entire device which, for a flow-battery, is dominated by the combined volume of the two electrolytes. Hence, rearranging eqn (11) for volume-flux of both electrolytes combined (i.e. $2F$) and introducing the energy density of the electrolyte leads to

$$\text{Power} = 2F\rho_e = 8\pi\Delta P kh\rho_e / \mu \ln[4a^2/r_w^2]. \quad (12)$$

Equation (12) is a key indicator of SFB performance. For example, a maximum safe excess pressure of 2 MPa, a permeability of 2D (=1.97×10^{-12} m^2), a reservoir thickness of 100m, an energy density of 277 MJ/m^3 (= 77 Wh L^{-1}, see earlier) a viscosity of 4×10^{-4} Pas (appropriate for a water-based electrolyte at 2km depth, (Likhachev 2003)), a well separation of 80 m (i.e. a=40m, see later for justification) and a bore-radius of 0.1m gives a power of 514 MW.

This is encouraging. For comparison, the London Array (the world's largest offshore wind-farm when completed in 2013) has a capacity of 630 MW. The SFB installation described above would therefore be capable of providing back-up of 81% of the maximum output from a wind-farm of London Array size.

Power-levels therefore look useful but the facility should also store sufficient energy to provide backup over an extended period. This capacity will be controlled by the size of subsurface containment structure and that will be site-specific. However, an order of magnitude estimate can be obtained from the time taken for electrolyte to travel from the injection well to the extraction well. This can be thought of as the time to "fill" or "empty" the reservoir since, after that time, partially (or fully) charged/discharged electrolyte will start to appear at the "wrong" well. In practice, the charge/discharge can continue beyond this point with little loss of performance since electrolyte will also be travelling along less direct routes. Hence, the minimum travel time provides a lower-limit for the true charge/discharge time.

The minimum time is found by restricting interest to the direct line between the source and sink so that eqn. (4) simplifies to

$$\Phi(x) = (Q/4\pi)\ \ln[\ (x+a)^2 / (x-a)^2\ ]. \qquad (13)$$

The velocity along this line is

$$u(x) = \partial\Phi / \partial x = Qa / \pi(a^2-x^2)$$

$$= Fa / \pi\varphi h(a^2-x^2) \qquad (14)$$

giving a travel time from source to sink of

$$t = \int_{-a}^{a} \frac{dx}{u}$$

$$= 4\pi\varphi h a^2 / 3F. \qquad (15)$$

Substitution of F, using eqn (11), allows eqn. (15) to be expressed as

$$t = (\varphi\mu a^2 / 3k\Delta P)\ \ln[\ 4a^2/r_w^2\ ]. \qquad (16)$$

Equation (16) gives a charge/discharge time of 20 hours for parameter-values as before and 10% porosity. Larger well separations increase this storage time. For example, a separation of 1 km (a=500m) would provide 180 days of charge/discharge, i.e. sufficient for seasonal balancing. However, as we'll show towards the end of this paper, storage on these longer time scales is more economically achieved by storing hydrogen gas whilst SFBs are more economic at storage times similar to those from PHS.

The volume capacity of the resulting system is obtained from a rearrangement of eqn. (15) to yield

$$Ft = 4\pi\varphi h a^2 / 3 \qquad (17)$$

with a corresponding energy capacity of

$$2Ft\rho_e = 8\pi\varphi h a^2 \rho_e / 3 \qquad (18)$$

Where the factor of 2 is introduced, as before, because the system is simultaneously pumping two electrolytes. For the same parameter-values as before, equation (18) yields a capacity of 10 GWh, i.e. similar to the PHS plant at Dinorwig (see earlier).

The implication of these preliminary results is that SFBs could provide electricity storage with sufficient charge/discharge power and sufficient energy-capacity to be useful. In addition, SFBs have a number of possible advantages over H_2 storage and CAES.

Firstly, the safety advantage already discussed (accidental leakage is environmentally benign) is enhanced by the near-constant storage-volume and temperature resulting from extracting charged (discharged) electrolyte whilst simultaneously injecting discharged (charged) electrolyte back into the same reservoir. This reduces the risk of containment failure since it avoids the thermo-mechanical stresses produced by the charge/discharge cycles of H_2 and CAES storage (e.g. see Böttcher et al., 2017 on H_2 storage in salt caverns). The negative relative pressure in the extraction half of the system also helps to maintain integrity.

Flow batteries can also have round-trip energy efficiencies (i.e. output energy/input energy) in excess of 80% (Tang *et al.* 2013). This compares favourably with <40% for H_2 electricity storage (Pfeiffer and Bauer 2015) and ~50% for existing CAES systems (Jafarizadeh *et al.* 2020) although it should be mentioned that adiabatic CAES may allow this to increase to >60% (Hartmann *et al.* 2012).

However, this high efficiency would be undermined if SFBs consumed significant energy in pumping viscous electrolytes through the porous subsurface. Note that energy-loss has the same units as ρ_e (i.e. energy loss for each m^3 of electrolyte pumped) and should be significantly smaller than ρ_e as we do not want to consume a significant fraction of the energy stored. Note also that energy densities have units of pressure ($J/m^3 \equiv Pa$) and, in fact, the pumping-loss energy density is simply the pressure drop from injection to extraction well. For the parameters used above, this is 4 MPa ($\equiv 4$ MJ/m^3, due to +2Mpa at injection and -2Mpa at extraction) compared with a storage energy density of 277 MJ/m^3. Hence, energy loss during pumping will reduce the round-trip efficiency by less than 3% (N.B. we are pumping two electrolytes and so total losses are 8 MJ/m^3).

A final theoretical advantage is the simplicity of SFBs. The same device is used for both charge and discharge and there are relatively few moving parts and no high-temperature components. Hence, SFBs are likely to be reliable, cheap to operate and relatively cheap to construct (see later for a more formal economic analysis).

In summary, SFBs look promising from power, storage-capacity, storage-time, safety, reliability and efficiency points of view. But these are theoretical expectations. In practice, there are significant hurdles to achieving this performance and we now turn to these.

A Preliminary Discussion of Possible Problems

This section takes a first look at issues that may make SFBs less effective than the foregoing analysis suggests or that may make SFBs too expensive to build. We start by estimating the size of flow-battery required to achieve the performance set out in section 2. Is it unrealistically large?

The size of any battery is controlled by the power collected/produced by each square metre of electrode during charging/discharging (the cell power density, not to be confused with the electrolyte energy density discussed earlier). Tucker et al (2015) give a value of 180 W/m^2 for their all-iron flow-battery. A practical device might therefore consist of banks of, say, 1kW cells each with an electrode area of ~5m^2. The thickness of each of these cells is hard to specify at present but is unlikely to differ greatly from ~0.1m to give each 1kW cell a volume of 0.56m^3. Hence, the SFB described in section 2, with a power output of 514 MW, would consist of cells with a total volume of 286 000 m^3. This could be contained in a cube of side 66m and is similar to the enclosed volume of the superstructure of an offshore oil-rig, i.e. it's challenging but not impossible. Furthermore, electrodes can be constructed with high surface areas (e.g. hierarchically structured electrodes, (Gabardo *et al.* 2013)) and these may allow substantial reductions in cell volume.

Higher power densities may also be possible. Gong et al. (2016) report all-iron flow-battery power densities of up to 1.6 kW/m^2 when using triethanolamine and cyanide anions in place of Cl^-. Unfortunately, these alternate anions have significant cost and environmental disadvantages and the order-of-magnitude improvement in volume only reduces device linear dimensions by a factor of two.

Another relevant factor is the possible need to cool the cells. This could require pumping of coolant with consequent increases in device volume and complexity. Fortunately, this does not appear to be an issue. If we assume the energy losses occur as low-grade heat which warms the electrolyte, then, from the definition of specific heat capacity, c, the expected warming, ΔT, is

$$\begin{aligned} \Delta T &= \Delta H / cM \\ &= 2\rho_e F(1-\eta)t / 2c\rho Ft \\ &= \rho_e(1-\eta) / c\rho \end{aligned} \quad (19)$$

where ΔH is heat input, M is mass, η is efficiency, and t is time. Assuming ρ_e=277 MJ/m^3, η=0.9 (10% energy losses on charging and 10% energy losses during discharging i.e. an 80% round-trip efficiency), c=4.2 kJ/K/kg and ρ=1000 kg/m^3 then gives ΔT=6.6K. This can easily be absorbed by the electrolytes; especially as they will have cooled from their subsurface values (~60 °C for a 2 km deep reservoir) as they were pumped up from depth and into the flow-cell.

The next problem we consider is that the maximum rate at which electrolyte can be pumped is constrained by the physics of porous reservoirs and so, to achieve high powers, the electrolyte must have high energy density. Unfortunately, achieved values are significantly lower than theoretical ones for the all-iron design. Tucker et al. (2015), for example, only achieved a density of 11.5 Wh/L (≡41.4 MJ/m^3)—a factor of 5 less than assumed in section 2. This brings the SFB estimated power down to 77 MW which may not be high enough to make such a system economic.

Yu et al. (2021) achieved a significantly better energy density of 32 Wh/L (≡115 MJ/m^3), using sulphate anions in place of chlorine, but this required addition of 1-ethyl-3-methylimidazolium chloride to enhance sulphate solubility. The cost and environmental implications of this requires further investigation.

Other ways forward, if energy densities are unavoidably low, is to increase the driving pressure and/or the reservoir permeability. There is some scope to increase pressure (e.g. by using deeper reservoirs) but this is ultimately limited by the efficiency issues discussed earlier; a 4 MPa pressure drop implies almost 20% energy losses due to pumping (if the energy density is only 41.4 MJ/m^3) and this deteriorates further as pressure is increased. An alternative approach is to increase permeability using hydraulic fracturing (Valkó 2014).

Another way to tackle issues of low energy density is simply to sink more wells, either into the same reservoir zone or, possibly, into a number of separate electrolyte ponds. This obviously increases costs. Horizontal drilling would also increase flow rates significantly (e.g. it has been used to obtain high rates of CO_2 injection at Sleipner (Kongsjorden *et al.* 1998)).

Hence, low energy density is unlikely to be an insuperable barrier to SFB deployment. Further research may bring energy densities up (current values are well below the theoretical maximum) and use of multiple wells, horizontal drilling and hydraulic fracturing should enable significant enhancements to the pumping rates given by the simplistic, single-source, single-sink, 2D modelling of section 2.

All the power and energy density issues, discussed to this point, will be important regardless of the flow-battery chemistry adopted. However, the all-iron configuration suffers from an additional, specific problem—"parasitic" hydrogen generation, i.e. generation of some hydrogen gas, instead of metallic iron, when reaction (2) is reversed. This reduces the round-trip efficiency of the cell but it will be supressed by the moderately high temperature of sub-surface stored electrolyte and can be supressed further by additives (Jayathilake *et al.* 2018). Another consequence of hydrogen production is the concomitant formation of insoluble iron hydroxide precipitate (Narayan, 2019) which may reduce reservoir permeability and which will reduce electrolyte concentration.

A more radical solution is to regard hydrogen generation as an opportunity rather than a problem! The SFB could be operated as a hybrid electrical-storage and H_2 generation device and, if a hydrogen-economy develops over the coming decades, selling parasitic hydrogen may be more cost-effective than preventing its generation. However, this would not solve the issue of iron hydroxide precipitation.

The subsurface nature of our proposed SFBs introduces a number of additional problems. The first is that electrolytes will inevitably be contaminated by contact with mineral surfaces, diluted by pore-fluids and metabolised by microbes in the subsurface. We need to determine whether these interactions will significantly reduce flow battery performance.

Some chemicals present may actually help (for example, NaCl is frequently used as a supporting electrolyte in flow batteries (e.g. Mundaray et al. (2021)) but other contaminants could result in unwanted side-reactions that consume reactants needed for reactions (1) and (2) or that lead to Fe loss and precipitates (e.g. iron oxides, hydroxide, and FeOOH) blocking pore-spaces and preventing electrolyte flow. However, some precipitates such as calcite or quartz may also be useful as they will predominantly form at the brine/electrolyte interface and, hence, help seal off the electrolyte from the brine. Detailed experimental investigations and geochemical modelling bringing electrolytes into contact with realistic brine chemistries and mineral surfaces will allow progress on understanding these issues.

Another major concern is electrolyte loss that depends on thermodynamic stability of injected $FeCl_3$ in formations waters. Wide variations in major ion and trace element chemistry are reported for the formation waters from the North Sea (see Warren et al., 1994) and quantifying the stability of aqueous $FeCl_3$ in every type of formation water is beyond the scope of this paper. Here, we illustrate this effect using a simplified idealised composition of formation water at equilibrium with the surrounding minerals reported from Sleipner field in the North Sea (Gauss et al., 2005) as this CO_2 storage location may also be suitable for electrolyte storage. This formation water has a pH of 7.67 and contains 3.5×10^{-8} M Al, 1.25×10^{-5} M Ba, 0.177 M Ca, 0.479 M Cl, 2.48×10^{-7} M Fe^{2+}, 1.4×10^{-4} M K^+, 0.011 M Mg^{2+}, 0.1 M Na^+, 4.5×10^{-4} M Si, and 2.5×10^{-4} M sulphate at 37 °C. Assuming no redox change and that the solution is in equilibrium with atmospheric CO_2 and contains no dissolved O_2, we calculate the aqueous speciation of ferric iron after injection of 6 M $FeCl_3$.

In our calculations, the solution becomes supersaturated with Fe-oxides (magnetite, hematite, maghemite) and -oxyhydroxides (lepidocrocite, goethite, ferrihydrite) above pH ~ 2.0. These preliminary calculations show a complete loss of the injected $FeCl_3$ at near-neutral pH, at which point precipitation of Fe-oxides and -oxyhydroxides also becomes extremely likely. Furthermore, additional loss of electrolyte takes place via hydrolysis of Fe^{3+} forming insoluble $Fe(OH)_3$, and via adsorption of Fe^{3+} onto mineral surfaces. In addition, when Fe speciation is calculated using a pe of -4.07 (Gauss et al., 2005), we observe a near complete loss of all Fe^{3+} between a pH range of 0.0 and 8.0. A detailed quantification of possible redox reactions relevant to North Sea formation waters is

beyond the scope of this article but future models should consider the effect of redox transformation of Fe and related electrolyte loss.

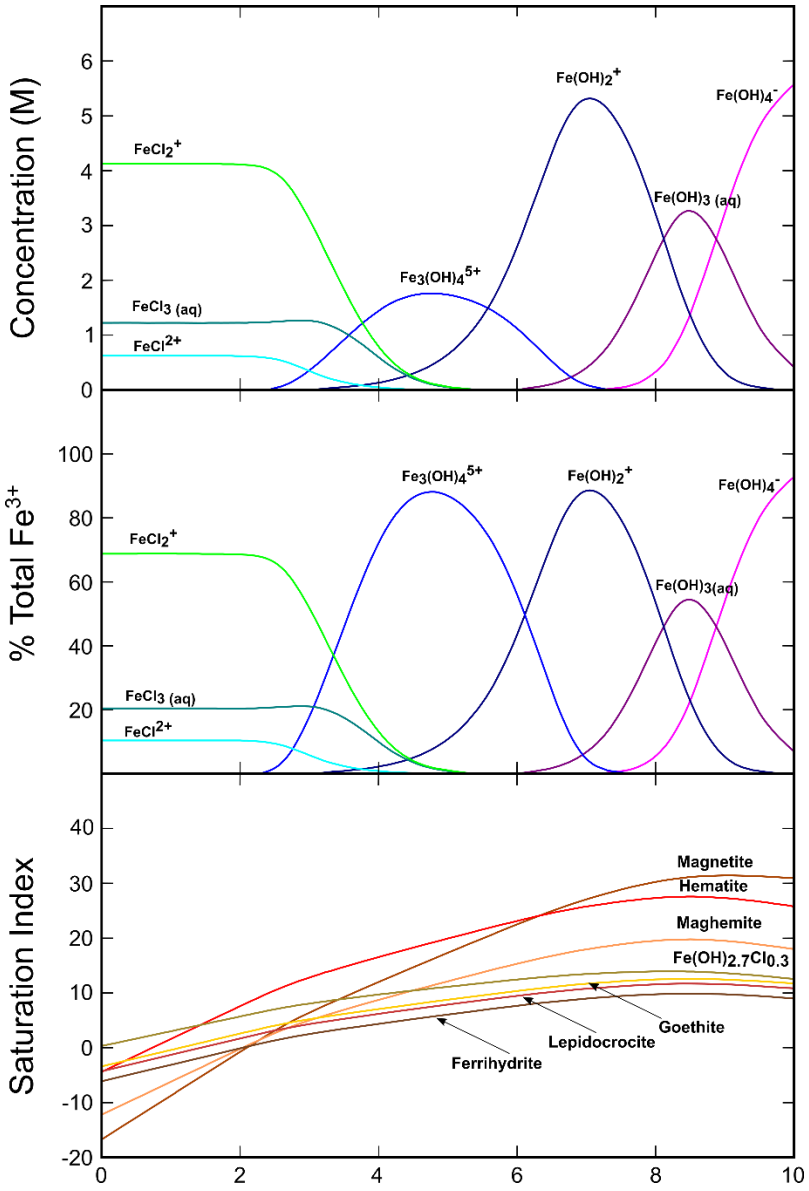

Figure 3. Aqueous speciation of Fe^{3+} phases in terms of concentration (top panel) and fraction of total Fe^{3+} (middle panel) in a solution similar to formation water at Sleipner field, North Sea (Gause et al., 2005). The concentration of Fe^{3+} is 6 M. The bottom panel shows the saturation index of iron oxide and oxy-hydroxide minerals with pH.

Microbes can also alter the electrolyte chemistry. In particular, charged electrolyte contains energy and is therefore a potential food-source (c.f. microbial contamination of stored H_2 (Zivar *et al.* 2021)). For example, in the presence of carbon compounds many anaerobic microbial communities "feed" by converting Fe(III) to Fe(II) (Chapelle 2001). Recently, microbial communities capable of reducing Fe^{3+} to Fe^{2+} have been identified in an oilfield (Vigneron et al., 2017). It has also been shown that naturally occurring strains of sulphur oxidising microbes can reduce aqueous $FeCl_3$ under acidic conditions (Brock and Gustafson, 1976). This would short-circuit reaction (1). We also need to consider the presence of produced hydrogen which may serve as an excellent electron donor for the

microbial metabolism, alter terminal electron accepting reactions, and stimulate biomass growth in the subsurface.

Hence, SFBs may suffer from microbially mediated self-discharge which could substantially reduce the useful storage duration and round-trip efficiency. Experiments are needed to quantify the severity of this problem as well as the extent to which it will be ameliorated by the moderately high temperature and salinity of the electrolytes. Experiments can also be undertaken to assess the effectiveness of "cleaning" the reservoir to remove carbon compounds.

A final consequence of bringing concentrated electrolytes into contact with natural brines is that it will lead to dilution through diffusive loss of ions. This will result in additional self-discharge and will require the electrolytes to be repeatedly "topped up", adding further costs. Precipitates at the brine/electrolyte interface may help prevent this problem and numerical modelling will allow its severity to be evaluated.

If electrolyte contamination and dilution are resistant to the solutions suggested above, they may instead be ameliorated by pre-flooding the reservoir with a non-reactive gas so that electrolytes are no longer in direct contact with native brine (Fig. 4). An exciting possibility would be to use CO_2 as this barrier, since SFBs could then also play a role in carbon-sequestration. The presence of CO2 would also lower the pH and, hence, help to suppress the generation of precipitates discussed above. However, using a barrier gas would require the reservoir to be sealed above as well as below and this would reduce the number of suitable locations.

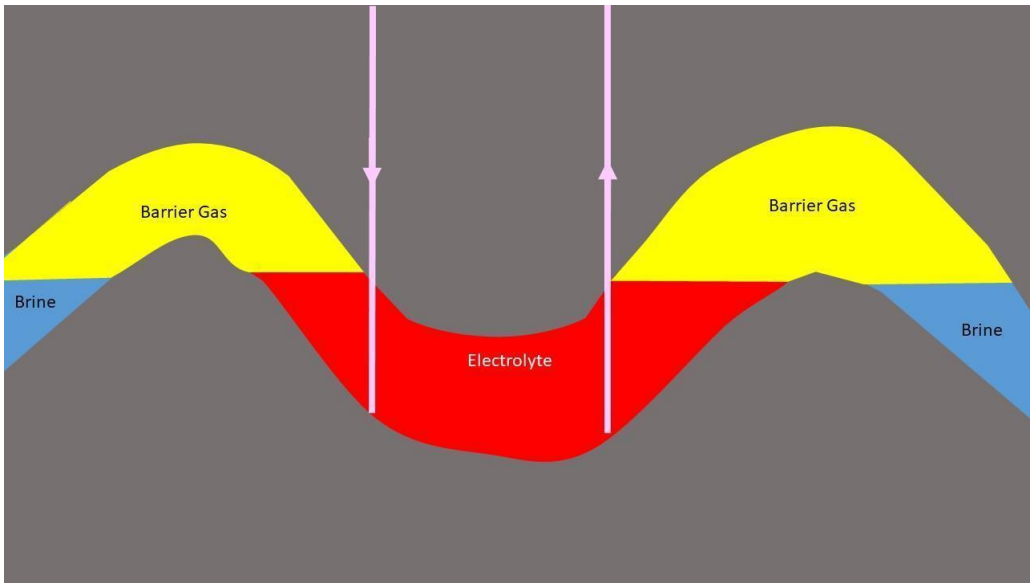

Figure 4. Protecting the electrolyte from contamination and diffusive ion-loss using a barrier gas (e.g. CO_2, N_2 or naturally present CH_4).

The fact that we plan to store electrolytes in porous media, rather than in well-mixed tanks, will also lead to novel problems. During charging we pump uncharged electrolyte out of one well whilst pumping-in charged electrolyte at another, spatially separate, well. The opposite happens during discharging (i.e. we reverse pumping direction so that discharged electrolyte is pumped into the uncharged electrolyte end of the reservoir). As a consequence, charged and discharged electrolytes are kept separate rather than being well mixed. Even after long-term use, there are likely to be significant ion-concentration gradients within the reservoirs. The consequences of this for flow-battery performance are unclear although it should help keep relevant ions at relatively high-concentrations and hence maintain high power levels. Laboratory experiments are needed to

investigate further and we propose to set up a laboratory all-iron cell with 4 tanks—one for charged anode electolyte, one for discharged anode electrolyte, one for charged cathode electrolyte and one for discharged cathode electrolyte—to determine how this separation affects performance.

Porous media additionally lead to the possibility that pore-spaces could become blocked by precipitates. This was mentioned earlier in the context of chemical contamination but precipitates can form even if there are no unwanted side-reactions since the iron deposited in reversed reaction (2) may not all be deposited on the electrode whilst the $FeCl_3$ involved in reaction (1) is a relatively low-solubility compound unless we operate the electrolyte at very low pH. Once again, laboratory work is required to evaluate the severity of these problems and to investigate possible solutions (e.g. additives and filters).

Furthermore, porous-rock storage leads to flow-rates (and hence power) being strongly constrained by electrolyte viscosity. The earlier calculations assumed that the electrolytes were sufficiently dilute that viscosity approximately equalled that of water. However, Yu *et al.* (2021) showed that the higher concentrations (2.2M) needed for good power (with iron sulphate electrolytes) led to a factor of 3 increase in viscosity. If a similar viscosity increase occurs in all-iron electrolytes too then it will reduce the power (but not the energy capacity) of the SFB by a factor of 3. Hence, we will need to determine the optimum compromise between energy density and viscosity when determining electrolyte concentrations. This requires further laboratory measurements.

A final set of problems, arising from sub-surface storage, is that the flow modelling of section 2 is highly simplistic and needs to be replaced with more realistic approaches. Sophisticated numerical models can investigate issues such as flow channelling (when flow becomes largely confined to a few, high permeability routes) and electrolyte trapping in cul-de-sacs (when electrolyte goes into an area but doesn't come out again). Both of these problems are well understood in the context of water-flooding of oil-fields to enhance recovery (e.g. Goudarzi et al. (2016)) and we anticipate that existing reservoir-modelling software will be able to investigate and evaluate the severity and impact of these problems.

We finish this section on potential problems with the need to obtain and retain public support. Given the oil industry's PR problems with hydraulic fracturing (Dodge and Metze 2017) and the fact that even wind-farms can be controversial (Ellis *et al.* 2007; Batel, 2020), it is likely that subsurface flow-batteries will meet resistance despite safety and environmental benefits. It is therefore necessary to discuss the technology openly and as widely as possible from an early stage. Issues that may affect acceptability relate to hydraulic fracturing, induced seismicity and contamination of ground water. Such considerations will also influence which locations are acceptable and may, for example, restrict development to offshore settings.

A First Look at Cost

Sub-surface flow batteries look promising. They can potentially provide high charge/discharge power for weeks to months and none of the technical challenges appear insurmountable. However, it is also important to consider whether SFBs are affordable.

We have neither the space nor the expertise for a full economic assessment, but we can take a first look at the energy installation cost. This is usually given in $/kWh and expresses the price of installing a given amount of storage capacity. Li-ion batteries, for example, cost $200/kWh to $1260/kWh (IRENA, 2017) whilst CAES ranges over €40-110/kWh (~$42-155/kWh) (Zakeri & Syri,

2015). PHS costs vary significantly depending upon location and size but IRENA (2017) quote an average of $25/kWh whilst Zakeri & Syri (2015) suggest €68/kWh (i.e. around $71/kWh).

Hence, if SFBs are to be an affordable alternative to PHS and CAES, the energy installation cost needs to be of the order of $50/kWh or less. We discuss the cost-comparison with hydrogen-storage in more detail a little later.

To estimate energy installation cost for an SFB, we use the fact that flow batteries decouple the system power from the system capacity. In traditional battery storage, both the power and the capacity are increased by adding cells whereas, in flow batteries, we increase power by adding more cells and increase capacity by adding more electrolyte. This separation of power from capacity allows the system cost to be divided into those that scale with the power (i.e. the cost of adding more or bigger stacks) and those that scale with capacity (i.e. the cost of increasing electrolyte volume).

For simplicity, in this first analysis, we assume that costs increase linearly with scale (as assumed also by others, e.g. see Mellentine (2011) and Yu et al (2021)). The overall installation cost is then

$$C = C_p P + C_e E \tag{20}$$

where C is cost, C_p is cost per unit power (for those components whose cost scales with power), P is power, C_e is cost per unit energy (for those components whose cost scales with the energy capacity) and E is energy capacity. In other words, C_p is the cost/kW for the stack whilst C_e is the cost/kWh for the tanks plus electrolytes.

The energy installation cost is, by definition, then

$$\frac{C}{E} = C_p \left(\frac{P}{E}\right) + C_e$$

$$= C_p T^{-1} + C_e. \tag{21}$$

where T is the storage duration defined as the time to fully charge or fully discharge the SFB at maximum power. With this background, we can investigate how well an SFB might perform economically.

Mellentine (2011) has estimated costs for a 10kW, 20.9kWh all-iron flow battery and these imply a cost for the stacks alone (i.e. without electrolytes, tanks and pumps) of $1338/kW. Alternatively, Yu et al (2021) put the stack cost at $135.1/m^2 which, combined with Tucker et al's (2015) power density estimate of 180W/m^2, implies $750/kW. In this section, we adopt the lowest price estimates because economies of scale are likely to push costs down significantly when flow batteries are used at grid-scale rather than the laboratory scale used in the papers we are getting costs from. Hence, we set C_p to $750/kW.

There are two main components to C_e: (i) the cost of storage tanks; (ii) the cost of electrolytes. In a wide-ranging review of the literature, Zakeri & Syri (2015) estimate hydrogen storage costs in tanks at $15/kWh and in geological storage at €0.25/kWh (~$0.26/kWh). However, the energy density of hydrogen is higher than that for flow-battery electrolytes. Taking the hydrogen energy density as 132 kWh/m^3 (Kabuth et al, 2017), compared to the SFB energy density of 77 kWh/m^3 used throughout this paper, implies that the storage costs will be 132/77=1.7 times higher, i.e. $26/kWh for surface storage and $0.45/kWh for underground storage.

Moving onto the electrolytes themselves, Mellentine (2011) estimated costs, for the electrolytes alone, at $21/kWh. Tucker et al (2015), on the other hand, report costs of $6.07/kWh whilst Yu et al

(2021) have an electrolyte cost of only \$3.37/kWh. As discussed above, we will use the lowest estimate.

Finally, for T, we use 20 hours as calculated earlier in this paper for the proposed 513MW, 10GWh SFB.

With these parameters, eqn (21) gives an energy installation cost of \$67/kWh for flow batteries with surface tanks and \$41/kWh if electrolytes are stored in the subsurface. These are encouraging cost estimates which would make flow battery storage about the same cost as CAES and pumped-hydro storage but with less severe geographical limitations.

The analysis can be extended to give estimates of the power installation cost which is usually given in \$/MW and expresses the price for a given charge/discharge power. This is particularly useful for comparing to costs of generators. For example, wind-turbines currently cost around \$1-2 million/MW and, ideally, we need storage power-costs to be smaller than this so that adding storage does not greatly increase the overall cost of wind-turbine power. As a benchmark, Zakeri and Syri (2015) estimate the power installation cost for PHS at €1.40 million/MW (~\$1.46 million/MW).

From eqn (20), the power installation cost is

$$\frac{C}{P} = C_e\left(\frac{E}{P}\right) + C_p$$

$$= C_eT + C_p \qquad (22)$$

which, with the parameters given above, yields a cost of \$1.3 million/MW for a system with surface tanks and \$0.8 million/MW for subsurface storage. Hence, the power installation cost also looks promising.

A similar analysis to that above can be carried out for hydrogen storage to allow a direct comparison. Schoenung (2011) gives the relevant figures for a hydrogen-based power to gas system as \$340/kW for the electrolyser, \$500/kW for the fuel cell (hence C_p=\$840/kW, a little higher than for SFBs) and \$0.3/kWh (much lower than for SFBs) for underground storage (=C_e since the cost of water can be assumed negligible).

The broad outline of this comparison is unlikely to change substantially as a consequence of future technical developments. Specifically, C_p will likely remain lower for SFBs than for H_2 because the latter approach requires both an electrolyser and a fuel-cell (or gas turbine) whereas energy storage and recovery are achieved using a single device in SFBs. The technologies behind electrolysers, fuel-cells and flow-batteries are similar and so C_p for SFB storage might conceivably become as little half the value for H_2 storage but is unlikely to get much smaller than that. In contrast, C_e will always be lower for H_2 storage than for SFB storage since the "feedstock" for H_2 storage is water at negligible cost. In addition, storage costs will always be lower for high-energy-density H_2 than for lower-energy-density electrolytes. Hence, we can be moderately confident that $C_{pf}<C_{ph}$ and $C_{eh}<C_{ef}$ will not change in the future (where C_{ph} is C_p for hydrogen storage, C_{pf} is C_p for flow battery storage, C_{ef} is C_e for flow battery storage and C_{eh} is C_e for hydrogen storage).

A consequence of this price structure is that there will be a storage duration below which SFB storage is cheaper than H_2 storage (or, equivalently, a storage duration above which H_2 storage will be cheaper than SFBs). The cross-over value of T can be found from either eqn (21) or (22) (which implies that the cross-over is identical for the energy installation price and the power installation price) and is given by

$$T = \frac{C_{ph} - C_{pf}}{C_{ef} - C_{eh}}. \quad (23)$$

Using the parameters given above, this predicts a cost-advantage for SFBs for T<26 hours. At the cross-over the energy installation prices are \$33/kWh and the power installation costs are \$0.85 million/MW, i.e. highly competitive with pumped hydroelectric storage.

Plausible improvements in SFB costs could take the cross-over T up to around 10-days but it is hard to envisage price-changes that could push the threshold much higher. It is therefore inevitable that H_2 storage will be economically advantaged for longer duration applications but SFBs could be superior for applications requiring storage times of less than a few days. In terms of the storage benefits listed in Table 1, SFBs are most likely to be useful for peaker replacement and for congestion management.

Conclusion

The first-approximation assessments made in this paper suggest that subsurface flow batteries (SFBs) may be able to provide safe electrical storage at high-power and low-cost. The costs are likely to be similar to those of CAES and PHS but with fewer geographical restrictions. Costs are also likely to be lower than for hydrogen-based power-to-gas storage in applications requiring storing less than a few-days of power. The SFB concept therefore warrants further investigation.

Author contributions

DW: Conceptualization (equal), formal analysis (lead), methodology (equal), original draft (lead), review and editing (equal), project administration (lead); **KH**: conceptualization (equal), methodology (equal), review and editing (equal); **AB**: conceptualization (equal), methodology (equal), review and editing (equal); **SK**: conceptualization (equal), methodology (equal), review and editing (equal); **NL**: formal analysis (supporting), review and editing (equal).

Data Availability Statement

Data sharing is not applicable to this article as no datasets were generated or analysed during the current study.

References

Alibaba. 2021. price of iron chloride, price of iron chloride Suppliers and Manufacturers at Alibaba.comhttps://www.alibaba.com/showroom/price-of-iron-chloride_2.html.

Batel, S., 2020. Research on the social acceptance of renewable energy technologies: Past, present and future. *Energy Research & Social Science*, **68**, https://doi.org/10.1016/j.erss.2020.101544.

Böttcher, N., Görke, U.-J., Kolditz, • Olaf and Nagel, T. 2017. Thermo-mechanical investigation of salt caverns for short-term hydrogen storage. *Environmental Earth Sciences*, **76**, https://doi.org/10.1007/s12665-017-6414-2.

Chapelle, F. 2001. Ground-water microbiology and geochemistry. 477.

Deane, J.P., Ó Gallachóir, B.P. and McKeogh, E.J. 2010. Techno-economic review of existing and new pumped hydro energy storage plant. *Renewable and Sustainable Energy Reviews*, **14**, 1293–1302, https://doi.org/10.1016/J.RSER.2009.11.015.

Dodge, J. and Metze, T. 2017. Hydraulic fracturing as an interpretive policy problem: lessons on energy controversies in Europe and the U.S.A. *http://dx.doi.org/10.1080/1523908X.2016.1277947*, **19**, 1–13, https://doi.org/10.1080/1523908X.2016.1277947.

Ellis, G., Barry, J. and Robinson, C. 2007. Many ways to say 'no', different ways to say 'yes': Applying Q-Methodology to understand public acceptance of wind farm proposals. *https://doi.org/10.1080/09640560701402075*, **50**, 517–551, https://doi.org/10.1080/09640560701402075.

EWE. 2017. EWE plans to build the world´s largest battery | EWE AGhttps://www.ewe.com/en/media/press-releases/2017/06/ewe-plans-to-build-the-worlds-largest-battery-ewe-ag.

Gabardo, C.M., Zhu, Y., Soleymani, L. and Moran-Mirabal, J.M. 2013. Bench-Top Fabrication of Hierarchically Structured High-Surface-Area Electrodes. *Advanced Functional Materials*, **23**, 3030–3039, https://doi.org/10.1002/ADFM.201203220.

Gong, K., Xu, F., Grunewald, J.B., Ma, X., Zhao, Y., Gu, S. and Yan, Y. 2016. All-Soluble All-Iron Aqueous Redox-Flow Battery. *ACS Energy Letters*, **1**, 89–93, https://doi.org/10.1021/ACSENERGYLETT.6B00049.

Goudarzi, A., Delshad, M. and Sepehrnoori, K. 2016. A chemical EOR benchmark study of different reservoir simulators. *Computers & Geosciences*, **94**, 96–109, https://doi.org/10.1016/J.CAGEO.2016.06.013.

Hartmann, N., Vöhringer, O., Kruck, C. and Eltrop, L. 2012. Simulation and analysis of different adiabatic Compressed Air Energy Storage plant configurations. *Applied Energy*, **93**, 541–548, https://doi.org/10.1016/J.APENERGY.2011.12.007.

Hruska, L.W. and Savinell, R.F. 1981. Investigation of Factors Affecting Performance of the Iron-Redox Battery. *Journal of The Electrochemical Society*, **128**, 18, https://doi.org/10.1149/1.2127366.

Huneke, F., Linkenheil, C.P. and Niggemeier, M. 2017. *KALTE DUNKELFLAUTE ROBUSTHEIT DES STROMSYSTEMS BEI EXTREMWETTER*.

IEA, 2009. Prospects for Large-Scale Energy Storage in Decarbonised Power Grids. International Energy Agency, https://www.osti.gov/etdeweb/servlets/purl/21248888.

690 IEA. 2020. Projected Costs of Generating Electricity 2020. International Energy Agency,
691 https://www.iea.org/reports/projected-costs-of-generating-electricity-2020.

692 IRENA, 2017. Electricity Storage and Renewables: Costs and Markets to 2030. International
693 Renewable Energy Agency, https://www.irena.org/-
694 /media/Files/IRENA/Agency/Publication/2017/Oct/IRENA_Electricity_Storage_Costs_2017.pdf.

695 Jafarizadeh, H., Soltani, M. and Nathwani, J. 2020. Assessment of the Huntorf compressed air energy
696 storage plant performance under enhanced modifications. *Energy Conversion and Management*,
697 **209**, 112662, https://doi.org/10.1016/J.ENCONMAN.2020.112662.

698 Jayathilake, B.S., Plichta, E.J., Hendrickson, M.A. and Narayanan, S.R. 2018. Improvements to the
699 Coulombic Efficiency of the Iron Electrode for an All-Iron Redox-Flow Battery. *Journal of The*
700 *Electrochemical Society*, **165**, A1630, https://doi.org/10.1149/2.0451809JES.

701 King Hubbert, M. 1957. (Print) (Online) Journal homepage: https://www.tandfonline.com/loi/thsj18
702 DARCY'S LAW AND THE FIELD EQUATIONS OF THE FLOW OF UNDERGROUND FLUIDS.
703 *Hydrological Sciences Journal*, **2**, 23–59, https://doi.org/10.1080/02626665709493062.

704 Kongsjorden, H., Karstad, O. and Torp, T.A. 1998. Saline aquifer storage of carbon dioxide in the
705 Sleipner project. *Waste Management*, **17**, 303–308, https://doi.org/10.1016/S0956-
706 053X(97)10037-X.

707 Likhachev, E.R. 2003. Dependence of Water Viscosity on Temperature and Pressure. *Translated from*
708 *Zhurnal Tekhnichesko oe Fiziki*, **48**, 135–136.

709 Mundaray, E., Sáez, A., Solla-Gullón, J. and Montiel, V. 2021. New insights into the performance of
710 an acid-base electrochemical flow battery. *Journal of Power Sources*, **506**, 230233,
711 https://doi.org/10.1016/J.JPOWSOUR.2021.230233.

712 Munz, I.A., Johansen, H., Huseby, O., Rein, E. and Scheire, O. 2010. Water flooding of the Oseberg
713 Øst oil field, Norwegian North Sea: Application of formation water chemistry and isotopic
714 composition for production monitoring. *Marine and Petroleum Geology*, **27**, 838–852,
715 https://doi.org/10.1016/J.MARPETGEO.2009.12.003.

716 Narayan, S., Nirmalchandar, A., Murali, A., Yang, B., Hoober-Burkhardt, L., Krishnamoorthy, S. and
717 Surya Prakash, G., 2019. Next-generation aqueous flow battery chemistries. *Current Opinion in*
718 *Electrochemistry* **18**, 72-80.

719 Park, M., Ryu, J., Wang, W. and Cho, J. 2016. Material design and engineering of next-generation
720 flow-battery technologies. *Nature Reviews Materials 2016 2:1*, **2**, 1–18,
721 https://doi.org/10.1038/natrevmats.2016.80.

722 Pfeiffer, W.T. and Bauer, S. 2015. Subsurface Porous Media Hydrogen Storage – Scenario
723 Development and Simulation. 1876–6102, https://doi.org/10.1016/j.egypro.2015.07.872.

724 Renewable Energy Agency, I. 2017. ELECTRICITY STORAGE AND RENEWABLES: COSTS AND MARKETS
725 TO 2030.

726 RWE. 2020. RWE researches large-scale storage for green electricity in salt
727 cavernshttps://www.rwe.com/en/press/rwe-gasstorage-west-gmbh/2020-09-30-rwe-
728 researches-large-scale-storage-for-green-electricity-in-salt-caverns.

729 Schmidt, O., Melchior, S., Hawkes, A. and Staffell, I., 2019. Projecting the Future Levelized Cost of
730 Electricity Storage Technologies. *Joule* **3**, 81-100.

731 Schoenung, S. M., 2011. Economic analysis of large-scale hydrogen storage for renewable utility
732 applications. United States Department of Energy, doi:10.2172/1029796.

733 Scottish Renewables. 2016. *The Benefits of Pumped Storage Hydro to the UK*.

734 Tang, A., McCann, J., Bao, J. and Skyllas-Kazacos, M. 2013. Investigation of the effect of shunt current
735 on battery efficiency and stack temperature in vanadium redox flow battery. *Journal of Power*
736 *Sources*, **242**, 349–356, https://doi.org/10.1016/J.JPOWSOUR.2013.05.079.

737 Tucker, M.C., Phillips, A. and Weber, A.Z. 2015. All-Iron Redox Flow Battery Tailored for Off-Grid
738 Portable Applications. *ChemSusChem*, **8**, 3996–4004, https://doi.org/10.1002/CSSC.201500845.

739 Valkó, P. 2014. Hydraulic Fracturing. *Kirk-Othmer Encyclopedia of Chemical Technology*, 1–24,
740 https://doi.org/10.1002/0471238961.HYDRVALK.A01.

741 Vigneron, A., Alsop, E. B., Lomans, B. P., Kyrpides, N. C., Head, I. M., and Tsesmetzis, N., 2017.
742 Succession in the petroleum reservoir microbiome through an oilfield production lifecycle. The
743 ISME Journal, 11, 2141-2154. https://doi.org/10.1038/ismej.2017.78.

744 Warren, E. A., Smalley, C. P., and Howarth, R. J., 1994. Part 4: Compositional variations of North Sea
745 formation waters. Geological Society, London, Memoirs, 15, 119-208.
746 https://doi.org/10.1144/GSL.MEM.1994.015.01.05

747 Weber, a., Mench, M., Meyers, J., Ross, P., Gostick, J and Liu, Q., 2011. Redox flow batteries: a
748 review. *J. Appl, Electrochem* **41**, DOI 10.1007/s10800-011-0348-2.

749 Yang, C-J., 2016. Pumped Hydrolectric Storage. *Storing Energy*, Letcher, T.M. (ed), Elsevier, 25-38.

750 Yu, S., Yue, X., Holoubek, J., Xing, X., Pan, E., Pascal, T. and Liu, P. 2021. A low-cost sulfate-based all
751 iron redox flow battery. *Journal of Power Sources*, **513**, 230457,
752 https://doi.org/10.1016/J.JPOWSOUR.2021.230457.

753 Zakeri. B. and Syri, S., 2015. Electrical energy storage systems: A comparative life cycle cost analysis.
754 *Renewable and Sustainable Energy Reviews,* **42**, 569-596.

755 Zivar, D., Kumar, S. and Foroozesh, J. 2021. Underground hydrogen storage: A comprehensive
756 review. *International Journal of Hydrogen Energy*, **46**, 23436–23462,
757 https://doi.org/10.1016/J.IJHYDENE.2020.08.138.